[12] A. Papoulis, *Signal Analysis*. New York: McGraw Hill, 1977, pp. 174–178.
[13] LJ. Stanković and S. Stanković, "Wigner distribution of noisy signals," *IEEE Trans. Signal Processing*, vol. 41, pp. 956–960, Feb. 1993.
[14] ——, "An analysis of instantaneous frequency representation using time frequency distributions—Generalized Wigner distribution," *IEEE Trans. on Signal Processing*, to be published.
[15] LJ. Stanković, "Wigner higher order spectra of multicomponent signals: A method for higher order time-frequency analysis," in *Proc. Int. Conf. DSP* (Nicosia, Cyprus), July 1993, pp. 100–105.

A General Procedure for the Derivation of Principal Domains of Higher-Order Spectra

Vinod Chandran and Steve Elgar

***Abstract*—A general procedure to determine the principal domain (i.e., nonredundant region of computation) of any higher-order spectrum is presented, using the bispectrum as an example. The procedure is then applied to derive the principal domain of the trispectrum of a real-valued, stationary time series. These results are easily extended to compute the principal domains of other higher-order spectra.**

I. Introduction

The primary purpose of this study is to provide a general procedure for deriving the principal domains (i.e., nonredundant regions) of higher-order spectra and use it to derive the nonredundant region of computation of the trispectrum. Higher-order spectra or polyspectra were introduced for studying nonlinearities and deviations from Gaussianity in stationary random processes. They are defined as the Fourier transforms of higher-order moments or cumulants of a random process. The idea of a spectral representation for higher-order moments of a time series appears in [1], and was further developed in [2]. A spectral representation for cumulants (attributed to Kolmogorov) appears in [2]. Higher-order spectra are derived from first principles in [3], [4]. For a single time series, the first higher-order spectrum is the (auto) power spectrum. The 2nd and 3rd higher-order spectra are the (auto) bispectrum and the (auto) trispectrum, and are defined as the Fourier transforms of the 3rd and 4th cumulants, respectively. Although cross higher-order spectra can be defined for multiple time series, the present study is restricted to a single time series and the prefix auto will be dropped. Further, it is not necessary to define higher-order spectra in terms of cumulants here. Instead, an alternative form involving products of Fourier coefficients of realizations of a random process will be used. This form can be derived from the cumulant based definition using Stieljes Integrals [4].

Manuscript received May 29, 1992; revised January 14, 1993. The associate editor coordinating the review of this paper and approving it for publication was Prof. Jose A. R. Fonollosa. This work was supported by the Office of Naval Research.

The authors have been with the School of Electrical Engineering and Computer Science, Washington State University, Pullman, WA 99164-2752. V. Chandran is now with the Signal Processing Research Centre, School of Electrical and Electronic Systems Engineering, Q.U.T., Brisbane, Queensland, Australia.

IEEE Log Number 9213287.

Let $x[t]$ be a real-valued, stationary random process. The bispectrum, $B(f_1, f_2)$, of the process can be expressed as

$$B(f_1, f_2) = E[X(f_1)X(f_2)X(-f_1 - f_2)] \tag{1}$$

where

$$x[t] = \int e^{j2\pi ft} dX(f)$$

is the Fourier decomposition of a realization of the process, * denotes complex conjugation, $j = \sqrt{-1}$, and $E[\,]$ is the expectation operator. This form of definition appears in [5] in an application of the bispectrum which precedes the theoretical development of cumulant spectra [3], [4]. Similarly, the trispectrum, $T(f_1, f_2, f_3)$, of the random process may be expressed as

$$T(f_1, f_2, f_3) = E[X(f_1)X(f_2)X(f_3)X(-f_1 - f_2 - f_3)]. \tag{2}$$

The bispectrum has been used in many applications including the study of quadratic interactions, signal reconstruction, system identification, and pattern recognition [7]. The trispectrum [4], [6], [8]–[11] has not enjoyed the same popularity as the bispectrum, partially because of the increased complexity in its computation and interpretation. Dalle Molle and Hinich [10] discuss part of the principal domain of the trispectrum. A procedure for the derivation of the complete principal domain is described in Section II, and applied to the bispectrum in Section III.

II. The Procedure

Let f denote the frequency normalized by the Nyquist frequency, such that $0 \leq f \leq 1$. If $x[t]$ is a real-valued time series, then the Fourier transform, $X(f)$, is conjugate symmetric, and hence $X^*(f) = X(-f)$. The bispectrum, $B(f_1, f_2)$, is then also given by

$$B(f_1, f_2) = E[X(f_1)X(f_2)X^*(f_1 + f_2)]. \tag{3}$$

The trispectrum or any other higher-order spectrum can also be expressed as the expected value of a product as in (3). The bispectrum (or other higher-order spectrum) possesses redundancy in bifrequency (or polyfrequency) space arising from

1) the interchangeability of any pair of frequencies in its definition (1),
2) redundancy of the negative half of some of the frequency axes owing to the conjugate symmetry property, and
3) periodicity of the Fourier transform at intervals of the sampling frequency for discrete-time processes.

This redundancy can be systematically exploited and eliminated to derive the principal domain or nonredundant region of computation of the bispectrum (or other higher-order spectrum). Thus, $B(f_1, f_2)$ need only be computed for a subset (derived here to illustrate the procedure) of all possible values of bifrequency (f_1, f_2).

Owing to property 1 the bispectrum is symmetric about the lines $f_1 = f_2$; $f_1 = -f_1 - f_2$ (or $2f_1 + f_2 = 0$); $f_2 = -f_1 - f_2$ (or $f_1 + 2f_2 = 0$) as shown in Fig. 1. The kth order polyspectrum will have $k(k+1)/2$ hyperplanes of symmetry in k-frequency space, analogous to the lines of symmetry above. The bispectrum need be computed only on one side of either of these lines, and therefore only for the subset

$$S_1^2 = \{f_1 \geq f_2\} \cap \{f_1 + 2f_2 \geq 0\} \tag{4}$$

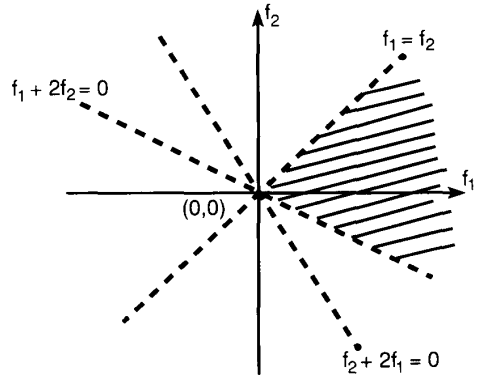

Fig. 1. The three lines of symmetry of the bispectrum arising from the interchangeability of the frequencies involved in its definition. The principal domain of the bispectrum must lie within the shaded region.

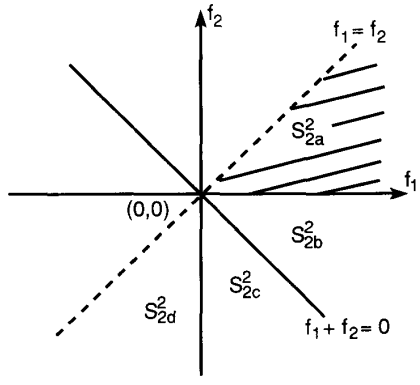

Fig. 2. The subsets into which bifrequency space is partitioned to exploit the redundancy arising from the conjugate symmetry property. The principal domain of the bispectrum must be contained in the shaded subset because all other subsets map into this subset.

which is shown shaded in Fig. 1. This subset for the kth order polyspectrum is

$$S_1^k = \{f_1 \geq f_2 \geq \cdots \geq f_k\} \cap \{f_1 + f_2 + \cdots + 2f_k \geq 0\}. \quad (5)$$

Property 2 must be exploited carefully because the redundancy involved is different for the trispectrum and other higher-order spectra than it is for the bispectrum, as will be evident in the next section. A systematic exploitation of this property consists of

- partitioning the k-frequency space into $2^{k+1} - 2$ subsets depending on the signs of the frequencies $f_1, f_2, \cdots, f_k$ and the sum frequency $f_1 + f_2 + \cdots + f_k$,
- grouping together all subsets that map into each other upon conjugate symmetric transformations, and
- including only one subset from each group in the nonredundant region.

Thus, for the bispectrum, bifrequency space can be partitioned into the six subsets, that (using the interchangeability property) can be rewritten as

$$S_{2d}^2 = \{f_1, f_2, f_s \geq 0\}$$
$$S_{2b}^2 = \{\text{exactly one frequency from } f_1, f_2 < 0; f_s \geq 0\}$$
$$S_{2c}^2 = \{\text{exactly one frequency from } f_1, f_2 < 0; f_s < 0\}$$
$$S_{2d}^2 = \{f_1, f_2, f_s < 0\}$$

where $f_s = f_1 + f_2$ and $f_1 \geq f_2$. These subsets are shown in Fig. 2. There are four unique subsets instead of six because the frequencies are ordered. The k-frequency space for the kth order polyspectrum can similarly be partitioned into $2k$ subsets (instead of $2^{k+1} - 2$) as

$$S_{2a}^k = \{f_1, f_2, \cdots, f_k, f_s \geq 0\}$$
$$S_{2b}^k = \{\text{exactly one frequency from } f_1, \cdots, f_k < 0; f_s \geq 0\}$$
$$S_{2c}^k = \{\text{exactly one frequency from } f_1, \cdots, f_k < 0; f_s < 0\}$$
$$S_{2d}^k = \{\text{exactly two frequencies from } f_1, \cdots, f_k < 0; f_s \geq 0\}$$
$$S_{2e}^k = \{\text{exactly two frequencies from } f_1, \cdots, f_k < 0; f_s < 0\}$$
$$\cdots = \cdots$$
$$S_{2x}^k = \{f_1, f_2, \cdots, f_k, f_s < 0\}$$

where $f_s = f_1 + f_2 + \cdots + f_k$ and $f_1 \geq f_2 \geq \cdots \geq f_k$. The redundancy among these subsets can now be eliminated using conjugate symmetry operations to test which subsets map into each other, as follows. Rearrange the equation $f_1 + f_2 + \cdots + f_k = f_s$ taking negative frequencies to the opposite side of the equation with a negation in sign until there are only sums of positive frequencies on each side. Each of the subsets, S_{2a}^k through S_{2x}^k can now be assigned a pair of integers of the form (l, r), where l and r are the number of frequencies on the left and right side of the equation, respectively, and $l + r = k + 1$. That is, S_{2d}^k is (k, l), S_{2b}^k is $(k - 1, 2)$, S_{2c}^k is $(k, 1)$, and so on. Those subsets that are assigned the same number pair will map into each other upon interchange of frequencies. In particular, S_{2c}^k will map to S_{2a}^k, S_{2e}^k will map to S_{2b}^k, S_{2g}^k will map to S_{2d}^k, etc. Thus, all the subsets with $f_s < 0$ can be eliminated. Further, (r, l) maps into (l, r) upon conjugation. This reduces the number of subsets that enter into the principal domain to $\lceil k/2 \rceil$ for the kth order polyspectrum. This formula yields only 1 region for the bispectrum (as is well known), but 2 regions for the trispectrum and 4-th order polyspectrum, 3 regions for the 5th- and 6th-order polyspectra, etc. Of these, S_{2a}^k will reduce to a sum interaction region, and the others will reduce to difference interaction regions for $k \geq 3$.

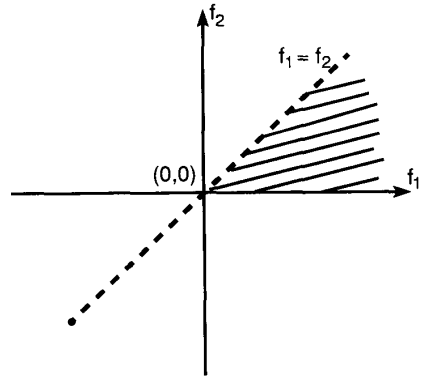

Fig. 3. The principal domain for the bispectrum of a continuous process is given by the shaded area.

Thus, only subset S_{2a}^2 need be retained for the bispectrum. Combining the two properties, the principal domain of computation of the bispectrum of a continuous process is given by $S_1^2 \cap S_{2a}^2$. This is the wedge shaped region shown in Fig. 3. For the kth order polyspectrum, there will be a similar wedge shaped sum interaction region. However, there are $\lceil k/2 \rceil - 1$ additional difference interaction regions as discussed in the next section.

Property 3 applies to discrete-time processes. Let $x[t]$ be sampled at time interval T. and normalize the frequencies by $f_N = 1/2T.X(f)$

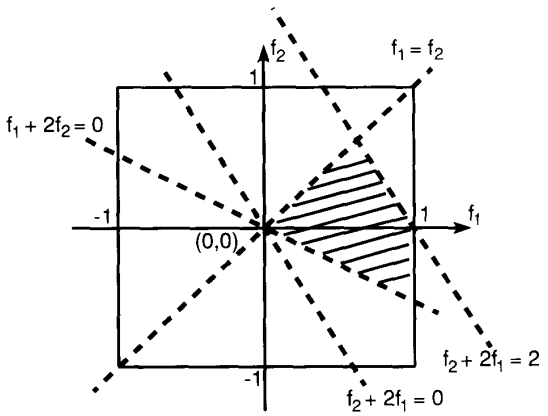

Fig. 4. The principal domain of the bispectrum of a discrete-time process must also be contained in the shaded region shown here because of the periodicity of the Fourier transform of a discrete-time function. The lines of symmetry of the bispectrum (shown in Fig. 1) also repeat periodically for the discrete-time bispectrum.

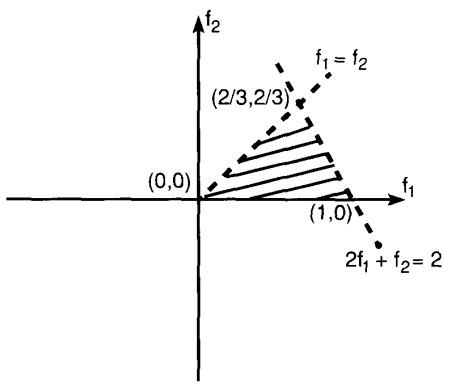

Fig. 5. The principal domain for the bispectrum of a discrete-time process is given by the shaded area.

is now periodic and uniquely defined in the interval $1 \geq f \geq -1$. More importantly, each of the lines (or hyperplanes) of symmetry will also be periodic at intervals of 2 units in normalized frequency. The bispectrum then need only be computed for the

$$S_3^2 = \{1 \geq f_1 \geq f_2 \geq -1\} \cap \{2 \geq 2f_1 + f_2 \geq 0\} \tag{6}$$

which is shown shaded in Fig. 4. The interchangeability property has also been utilized in (6) to order the frequencies. This subset for the kth order polyspectrum would be

$$S_3^k = \{1 \geq f_1 \geq f_2 \geq \cdots \geq f_k \geq -1\} \cap \{2 \geq 2f_1 + f_2 + \cdots + f_k \geq 0\}. \tag{7}$$

Combining all three properties, the principal domain of the bispectrum for a discrete-time process is given by $S_1^2 \cap S_{2a}^2 \cap S_3^2$, which is the triangular region shown in Fig. 5.

For a continuous-time bandlimited process with unit bandwidth in normalized frequency, or for a discrete-time process when there is no polyspectral aliasing [4], the subset S_3 comprises a smaller region given by

$$S_{3IT}^2 = \{1 \geq f_1 \geq f_2 \geq -1\} \cap \{1 \geq f_1 + f_2 \geq -1\}. \tag{8}$$

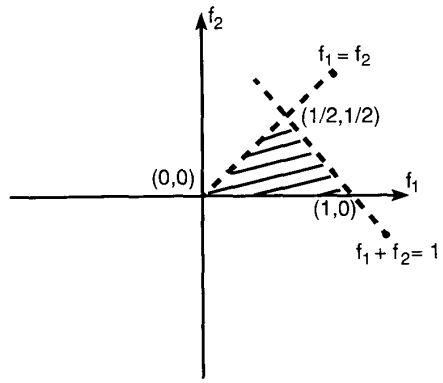

Fig. 6. The principal domain for the bispectrum of a continuous-time bandlimited process with unit bandwidth in normalized frequency units is given by the shaded area. This is also the principal domain for the bispectrum of a discrete-time process with no bispectral aliasing.

For the kth order polyspectrum this subset is given by

$$S_{3IT}^k = \{1 \geq f_1 \geq f_2 \cdots \geq f_k \geq -1\} \cap \{1 \geq f_1 + f_2 + \cdots + f_k \geq -1\}. \tag{9}$$

The principal domain of the bispectrum for a continuous-time bandlimited process with unit bandwidth in normalized frequency or for a discrete-time process with no polyspectral aliasing is given by the shaded triangular region shown in Fig. 6. The difference between the two shaded triangular regions in Figs. 5 and 6 is known as the outer triangle or OT region [7], and it has its k-dimensional counterpart for the kth order polyspectrum.

III. Principal Domain of the Trispectrum

The procedure described above is now applied to the trispectrum. Using the interchangeability of frequencies, the planes of symmetry of the trispectrum are $f_1 = f_2$; $f_2 = f_3$; $f_1 = f_3$; $2f_1 + f_2 + f_3 = 0$; $f_1 + 2f_2 + f_3 = 0$; and $f_1 + f_2 + 2f_3 = 0$. The principal domain must therefore be contained in

$$S_1^3 = \{f_1 \geq f_2 \geq f_3\} \cap \{f_1 + f_2 + 2f_3 \geq 0\}. \tag{10}$$

Using the conjugate symmetry property, the trifrequency space can be partitioned into the subsets

$$S_{2a}^3 = \{f_1, f_2, f_3, f_s \geq 0\}$$
$$S_{2b}^3 = \{\text{exactly one frequency from } f_1, f_2, f_3 < 0 \text{ and } f_s \geq 0\}$$
$$S_{2c}^3 = \{\text{exactly one frequency from } f_1, f_2, f_3 < 0 \text{ and } f_s < 0\}$$
$$S_{2d}^3 = \{\text{exactly two frequencies from } f_1, f_2, f_3 < 0 \text{ and } f_s \geq 0\}$$
$$S_{2e}^3 = \{\text{exactly two frequencies from } f_1, f_2, f_3 < 0 \text{ and } f_s < 0\}$$
$$S_{2f}^3 = \{f_1, f_2, f_3, f_s < 0\}$$

where $f_s = f_1 + f_2 + f_3$. Denoting subsets S_{2a}^3 through S_{2f}^3 by integer pairs (as explained above), they are found to be (3, 1), (2, 2), (3, 1), (1, 3), (2, 2), and (1, 3), respectively. After eliminating identical and commuted pairs, only subsets S_{2a}^3 and S_{2b}^3 remain for inclusion in the principal domain.

Combining the two properties, the principal domain of the trispectrum for a continuous process is given by $S_1^3 \cap (S_{2a}^3 \cap S_{2b}^3)$. The contribution from S_{2b}^3 is a *difference interaction* region which does not reduce to cubic sum interactions. This is a significant difference between the principal domains of the bispectrum and the trispectrum.

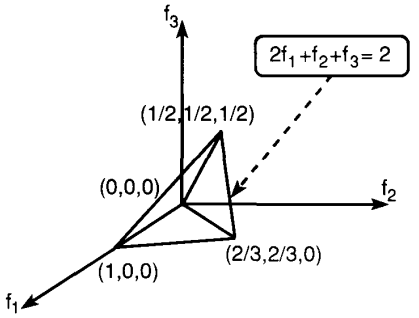

Fig. 7. The sum interaction region, T_1, which forms part of the principal domain of the discrete-time trispectrum.

For a discrete-time process, using the periodicity property, the trispectrum need only be computed in the subset

$$S_3^3 = \{1 \geq f_1 \geq f_2 \geq f_3 \geq -1\} \cap \{2 \geq 2f_1 + f_2 + f_3 \geq 0\}. \quad (11)$$

The principal domain of the discrete-time trispectrum is given by $S_1^3 \cap (S_{2a}^3 \cap S_{2b}^3) \cap S_3^3$. It comprises the sum interaction region, $T_1 = S_1^3 \cap S_{2a}^3 \cap S_3^3$ shown in Fig. 7 and the difference interaction region, $T_2 = S_1^3 \cap S_{2b}^3 \cap S_3^3$ shown in Fig. 8. In terms of the frequencies, f_1, f_2, f_3,

$$\begin{aligned} T_1 &= \{f_1 \geq f_2 \geq f_3\} \cap \{f_1 + f_2 + 2f_3 \geq 0\} \\ &\quad \cap \{f_1 \geq 0, f_2 \geq 0, f_3 \geq 0\} \\ &\quad \cap \{1 \geq f_1 \geq f_2 \geq f_3 \geq -1\} \\ &\quad \cap \{2 \geq 2f_1 + f_2 + f_3 \geq 0\} \\ &= \{1 \geq f_1 + f_2/2 + f_3/2 \geq f_1 \geq f_2 \geq f_3 \geq 0\} \end{aligned} \quad (12)$$

where the constraint $f_1 + f_2 + 2f_3 \geq 0$ is ignored because it is dominated by the stronger constraint $f_3 \geq 0$. This is a tetrahedron with vertices (found by solving equalities simultaneously in the defining relations for T_1) at (0, 0, 0), (1, 0, 0), (2/3, 2/3, 0), and (1/2, 1/2, 1/2) as shown in Fig. 7. Similarly,

$$\begin{aligned} T_2 &= \{f_1 \geq f_2 \geq f_3\} \cap \{f_1 + f_2 + 2f_3 \geq 0\} \\ &\quad \cap \{f_1, f_2 \geq 0 \geq f_3\} \cap \{f_1 + f_2 + f_3 \geq 0\} \\ &\quad \cap \{1 \geq f_1 \geq f_2 \geq f_3 \geq -1\} \\ &\quad \cap \{2 \geq 2f_1 + f_2 + f_3 \geq 0\} \\ &= \{1 \geq f_1 \geq f_2 \geq 0 \geq f_3 \geq -1\} \\ &\quad \cap \{2 \geq 2f_1 + f_2 + f_3\} \\ &\quad \cap \{f_1 + f_2 + 2f_3 \geq 0\} \end{aligned} \quad (13)$$

where the constraint $f_1 + f_2 + f_3 \geq 0$ is ignored because it is dominated by the stronger constraint $f_1 + f_2 + 2f_3 \geq 0$ when f_3 is negative. This is a polyhedron with vertices (found by solving equalities simultaneously in the defining relations for T_2) at (0, 0, 0), (1, 0, 0), (2/3, 2/3, 0), $(1, 0, -1/2)$ and $(1, 1, -1)$ as shown in Fig. 8. This region has not been reported previously.

For a continuous-time bandlimited process with unit bandwidth in normalized frequency, or for a discrete-time process with no trispectral aliasing, the subset S_3^3 comprises a smaller region given by

$$S_{3IT} = \{1 \geq f_1 \geq f_2 \geq f_3 \geq -1\} \cap \{1 \geq f_1 + f_2 + f_3 \geq -1\}. \quad (14)$$

Thus, the principal domain of the trispectrum for a continuous-time bandlimited process with unit bandwidth in normalized frequency or for a discrete-time process with no trispectral aliasing, consists of

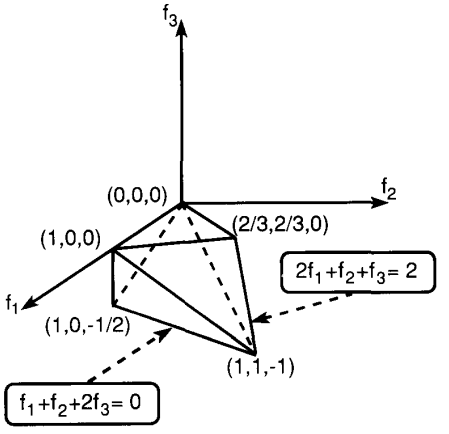

Fig. 8. The difference interaction region, T_2, which also forms part of the principal domain of the discrete-time trispectrum.

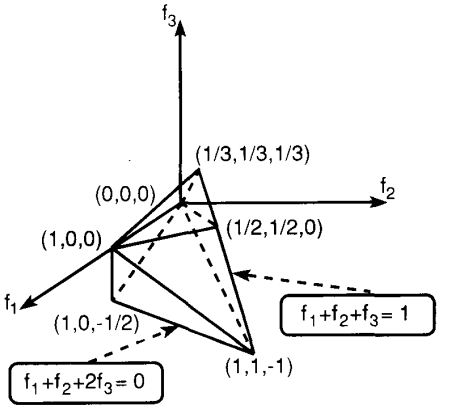

Fig. 9. The principal domain of the trispectrum for a continuous-time, bandlimited process with unit bandwidth in normalized frequency units. This is also the principal domain of the discrete-time trispectrum with no trispectral aliasing.

smaller regions as shown in Fig. 9. These regions are T_1 and T_2, where

$$T_1 = \{1 \geq f_1 + f_2 + f_3 \geq f_1 \geq f_2 \geq f_3 \geq 0\} \quad (15)$$

which is a tetrahedron with vertices at (0, 0, 0), (1, 0, 0), (1/2, 1/2, 0), (1/3, 1/3, 1/3), and

$$\begin{aligned} T_2 &= \{1 \geq f_1 \geq f_2 \geq 0 \geq f_3 \geq -1\} \\ &\quad \cap \{f_1 + f_2 + 2f_3 \geq 0\} \cap \{1 \geq f_1 + f_2 + f_3\} \end{aligned} \quad (16)$$

which is a polyhedron with vertices at (0, 0, 0), (1, 0, 0), (1/2, 1/2, 0), $(1, 0, -1/2)$ and $(1, 1, -1)$.

The principal domain of the kth order polyspectrum comprises $\lceil k/2 \rceil$ regions given by

$$T_1^k = \{1 \geq f_1 + f_2 + \cdots + f_k \geq f_1 \geq f_2 \cdots \geq f_k \geq 0\} \quad (17)$$

$$\begin{aligned} T_2^k &= \{1 \geq f_1 \geq f_2 \geq \cdots \geq f_{k-1} \geq 0 \geq f_k \geq -1\} \\ &\quad \cap \{f_1 + f_2 + \cdots + 2f_k \geq 0\} \\ &\quad \cap \{1 \geq f_1 + f_2 + \cdots + f_k\} \end{aligned} \quad (18)$$

$$\begin{aligned} T_3^k &= \{1 \geq f_1 \geq f_2 \geq \cdots \geq f_{k-2} \geq 0 \geq f_{k-1} \geq f_k \geq -1\} \\ &\quad \cap \{f_1 + f_2 + \cdots + 2f_k \geq 0\} \\ &\quad \cap \{1 \geq f_1 + f_2 + \cdots + f_k\} \end{aligned} \quad (19)$$

and so on. These regions may be combined into one as done for the trispectrum in Fig. 9.

IV. Conclusions

A procedure applicable to all higher-order spectra was used to derive the nonredundant region of computation of the trispectrum. This region differs from that derived by a direct extension of the principal domain of the bispectrum to three dimensions.

References

[1] A. Blanc-Lapierre and R. Fortet, *Theorie des Fonctions Aleatoires*. Paris: Masson, 1953.

[2] A. N. Shiryaev, "Some problems in the spectral theory of higher order moments," *Theor. Prob. Appl.*, vol. 5, pp. 265–284, 1960.

[3] D. R. Brillinger, "An introduction to polyspectra," *Ann. Math. Stat.*, vol. 36, pp. 1351–1374, 1965.

[4] D. R. Brillinger and M. Rosenblatt, "Computation and interpretation of kth order spectra," B. Harris, *Spectral Analysis of Time Series*. New York: Wiley, 1967, pp. 189–232.

[5] K. Hasselmann, W. Munk, and G. MacDonald, "Bispectra of ocean waves," in M. Rosenblatt, Ed. *Time Series Analysis*. New York: Wiley, 1963, pp. 48–69.

[6] K. S. Lii and M. Rosenblatt, "A fourth order deconvolution technique for nonGaussian linear processes," P. R. Krishnaiah, *Multivariate Analysis VI*. Amsterdam, The Netherlands: Elsevier, 1985, pp. 395–410.

[7] C. L. Nikias and M. R. Raghuveer, "Bispectrum estimation: A digital signal processing framework," *Proc. IEEE*, vol. 75, pp. 869–891, 1987.

[8] R. F. Dwyer, "Fourth-order spectra of sonar signals," *Proc. Workshop Higher-Order Spectral Analysis*, Vail, CO, 1989, pp. 52–55.

[9] A. S. Marathay, Y. Hu, and P. S. Idell, "Object reconstruction using third and fourth order intensity correlations," *Proc. Workshop Higher-order Spectral Analysis*, pp. 124–129, Vail, CO, 1989.

[10] J. W. Dalle Molle and M. J. Hinich, "The trispectrum," *Proc. Workshop on Higher-order Spectral Analysis*, Vail, CO, 1989, pp. 68–72.

[11] L. D. Lutes and D. C. K. Chen, "Trispectrum for the response of a nonlinear oscillator," *Int. Journal of Nonlinear Mechanics*, vol. 26, no. 6, pp. 893–909, 1991.

The Effect of Source Number Underestimation on MUSIC Location Estimates

Bill M. Radich and Kevin M. Buckley

***Abstract*—An analytical expression for the variance of MUSIC source location estimates is derived under the assumption that the detection step has already taken place, resulting in an underestimation of the source number. The analytic predictions are compared with Monte-Carlo simulation results for beam-space MUSIC. The derived variance expression is more general than those reported to date and is also valid for other situations where the asymptotic correlation matrix yields biased source estimates.**

Manuscript received January 25, 1993. The associate editor responsible for coordinating the review of this paper and approving it for publication was Prof, Georgios B. Giannakis

The authors are with the Department of Electrical Engineering, University of Minnesota, Minneapolis, MN 55455. This research was supported by ONR under contract N00014-90-J-1049 and NSF.

IEEE Log Number 9213297.

I. Introduction

One of the most challenging problems encountered in the practical application of statistical estimation techniques to real-world data is the determination of an appropriate model dimension based only on the observed data. Although a number of investigations concerning the characteristics of eigenstructure-based direction of arrival (DOA) estimates have been recently reported [1]–[3], the exact number of impinging sources has always been assumed known *a priori*. Here, it is assumed that the detection step has already taken place, resulting in the incorrect estimate of $\tilde{D}$ sources, and therefore, the detection problem shall not be covered in any detail. As will be explained in the Section III-A, the case of overestimating the number of signals can be analyzed as a special case of weighted MUSIC, and therefore, variance analysis falls within the framework of results published in [3].

In this study, we are concerned with the effects that *underestimating* the number of narrowband sources D impinging on an array of sensors has on the source estimates. Specifically, the variance of MUSIC [5] source location estimates is derived when it is assumed that there are $\tilde{D}$ sources, with $\tilde{D} < D$. We note that a more general formulation of the problem has been addressed independently in [4].

Of course, if there are really two impinging sources and the MUSIC spectrum is computed under the assumption that there is only one, a single source estimate may or may not be meaningful. For instance, if the two sources are equipowered, at a relatively high SNR, and well separated in space, a single source estimate would not give any reasonable degree of accuracy for either of the sources. However, in such a situation, it is also highly unlikely that *any* of the standard detection methods would fail to detect both sources. Therefore, from a practical standpoint, the variance expressions derived here are appropriate for many realistic situations.

II. Background

Consider D narrowband, far-field, and noncoherent signals radiating from source locations $\theta_1, \theta_2, \ldots, \theta_D$. The sources impinge on an array of K sensors. Denote the array response vector corresponding with each source location θ_i as $a(\theta_i)$. The $K \times 1$ array observation vector is therefore modeled as

$$x(t) = As(t) + n(t). \tag{1}$$

where A is the $K \times D$ array response matrix, and $s(t)$ is the $D \times 1$ signal vector that is assumed to be uncorrelated with the $K \times 1$ noise vector. The signal and noise processes are modeled as temporally white and zero-mean complex Gaussian processes with $E\{s(t)s^H(t)\} = P_s$ and $E\{n(t)n^H(t)\} = \sigma^2 I_K$. Here, P_s is assumed full rank, and the superscript 'H' denotes the complex conjugate transpose. Throughout this paper, the superscripts '$*$' and 'T' shall denote the operations of complex conjugation and transpose, respectively. The covariance matrix of the observation vector is thus

$$E\{x(t)x^H(t)\} = R_x = AP_sA^H + \sigma^2 I_K. \tag{2}$$

Let $(\lambda_1, \lambda_2, \ldots, \lambda_K)$, and $(e_1, e_2, \ldots, e_K)$ represent the sets of ordered eigenvalues and corresponding eigenvectors of R_x, where $\lambda_1 \geq \lambda_2 \geq \ldots \geq \lambda_K$. The ranges of the $K \times D$ matrix $E_s = [e_1, e_2, \ldots, e_D]$, and the $K \times (K - D)$ matrix $E_n = [e_{D+1}, \ldots, e_K]$ are commonly referred to as the signal and noise subspaces, respectively. In practice, R_x is often estimated from the